Available online at www.sciencedirect.com
SCIENCE DIRECT
Science Press
Trans. Nonferrous Met. Soc. China 16(2006) 747−752
Transactions of Nonferrous Metals Society of China
www.csu.edu.cn/ysxb/

Hydrogen desorption kinetics of amorphous $Mg_{0.9}Ti_{0.1}Ni_{1-x}Pd_x$ (x=0, 0.05, 0.1 and 0.15) electrode alloys

TIAN Qi-feng(田琦峰)[1, 2], ZHANG Yao(张 耀)[1], TAN Zhi-cheng(谭志诚)[1],
XU Fen(徐 芬)[1], SUN Li-xian(孙立贤)[1], YUAN Hua-tang(袁华堂)[3]

1. Dalian Institute of Chemical Physics, Chinese Academy of Sciences, Dalian 116023, China;
2. Graduate School, Chinese Academy of Sciences, Beijing 100049,China;
3. Institute of New Energy Material Chemistry, Nankai University, Tianjin 300071, China

Received 20 September 2005; accepted 7 April 2006

Abstract: The amorphous $Mg_{0.9}Ti_{0.1}Ni_{1-x}Pd_x$ (x=0, 0.05, 0.1, 0.15) hydrogen storage alloys were prepared by mechanical alloying. The hydrogen desorption kinetics of the electrode alloys were studied by potentiostatic discharge experiments and linear polarization measurements. The experimental results show that the three-dimensional diffusion model dominates the hydrogen desorption process of the electrode alloys. The rate constants of hydrogen desorption reaction, which are obtained from a linear fitting of the model equation, increase with temperature. The activation energies of hydrogen desorption were calculated according to the Arrhenius equation. The calculated values were 46.2, 24.29, 33.4 and 34.95 kJ/mol for x=0, 0.05, 0.1 and 0.15 of $Mg_{0.9}Ti_{0.1}Ni_{1-x}Pd_x$ (x=0, 0.05, 0.1, 0.15) electrode alloys, respectively. The exchange current densities were determined by the linear polarization experiments. The variation of exchange current densities with Pd content in the alloy electrodes agrees with that of activation energies with Pd content.

Key words: hydrogen desorption kinetics; potentiostatic discharge; three-dimensional diffusion; activation energy; hydrogen storage alloys

1 Introduction

Mg-based alloy is a kind of promising hydrogen storage materials used for fuel cell. It is also a potential candidate as cathode materials of Ni-MH rechargeable batteries due to its large discharge capacity[1]. However, its cyclic stability is not satisfactory yet because Mg is oxidized easily in KOH solution. Many methods, such as element substitution, were used to improve its cyclic stability[2,3]. Recently some work focused on the substitution of Ti for Mg to prolong the cycle life of electrode alloys[4−7].

It was found that the additional Pd in the MgNi alloy effectively improved its corrosion inhibition performances and cyclic stability[8,9]. In our previous work, the further substitution of Pd for Ni was also demonstrated to enhance the cyclic stability of amorphous $Mg_{0.9}Ti_{0.1}Ni_{1-x}Pd_x$ (x=0, 0.05, 0.1, 0.15) hydrogen storage alloys[10].

Hydrogen storage capacity and hydrogen absorption/desorption kinetics are the crucial properties for hydrogen storage materials[11−16]. As we know, the isothermal tests on hydrogen absorption/desorption kinetics can be performed in electrochemical system, which is an open system and the reaction heat is easily transferred in alkaline aqueous solution. Moreover, the electrochemical reaction can be readily controlled at a constant applied potential, which corresponds to a certain hydrogen equilibrium pressure of the electrode alloys. NORTHWOOD et al[17] studied the hydrogen desorption kinetics of $LaNi_{4.7}Al_{0.3}$ electrode alloy by means of potentiostatic measurements at various applied potentials and temperatures. They found that phase transformation ($\beta \rightarrow \alpha$) controlled the hydrogen desorption of the $LaNi_{4.7}Al_{0.3}$ electrode within the temperature range from 289 K to 328 K and the applied potential range from −0.80 to −0.60 V (vs Hg/HgO electrode).

However, the hydrogen desorption kinetics of Mg-based hydrogen storage electrode alloy is rarely studied up to now. In this paper, the hydrogen desorption

Foundation item: Projects(20373072, 20473091) supported by the National Natural Science Foundation of China
Corresponding author: TAN Zhi-cheng; Tel: +86-411-84379199; E-mail: tzc@dicp.ac.cn

kinetics of $Mg_{0.9}Ti_{0.1}Ni_{1-x}Pd_x$ (x=0, 0.05, 0.1, 0.15) electrode alloys were investigated by means of potentiostatic discharge technique. The linear polarization tests were adapted to verify the kinetic results obtained from potentiostatic discharge measurements.

2 Experimental

$Mg_{0.9}Ti_{0.1}Ni_{1-x}Pd_x$ (x=0, 0.05, 0.1, 0.15) alloys were prepared by mechanical alloying(MA). The purity of all metallic powders was higher than 99.5%. The metallic powders with designed stoichiometry were ground in a planetary mill with a ball to powder mass ratio of 30:1 under Ar atmosphere for 120 h. The structures of the alloys were characterized by X-ray diffraction(XRD, Rigaku D/max-2500, CuK_α, 50 kV, 200 mA) and transmission electron microscopy (TEM, Philips F-20 TECNAI G^2, 200 kV).

The working electrode materials to be tested were the pressed mixture of 0.1 g alloy powder with 0.3 g electrolytic Cu powder. The NiOOH/$Ni(OH)_2$ electrode and Hg/HgO electrode were used as a counter electrode and a reference one, respectively. The electrolyte was 6 mol/L KOH aqueous solution. A Luggin capillary tube, which was connected to the reference electrode, was close to the working electrode to minimize the ohmic drop across the electrolyte solution. The charge-discharge tests were performed upon an automatic LAND battery test instrument. The electrodes were charged for 3 h at a current density of 300 mA/g and then discharged at a current density of 100 mA/g until 50% depth of discharge(DOD). The potentiostatic discharge and linear polarization measurements were conducted on the Zahner Elektrik IM6e electrochemical workstation. The discharge tests were executed at the end of charge. The applied potential for discharge experiments was −0.7 V (vs Hg/HgO electrode). The discharge temperatures were 298, 303 and 313 K, respectively. For each test, the discharge current was recorded as a function of time. The tests were terminated when the discharge current was less than 1 mA. The linear polarization curves were measured from −5 mV to 5 mV (vs open circuit potential) with a scanning rate of 0.1 mV/s at 50% DOD and 303 K.

3 Results and discussion

3.1 Phase structure of alloys

Fig.1 shows the X-ray diffraction patterns of $Mg_{0.9}Ti_{0.1}Ni_{1-x}Pd_x$ (x=0, 0.05, 0.1, 0.15) quaternary alloys after ball milling for 120 h. For each alloy, a broad Bragg peak was observed at approximately 42° (2θ). No peak of secondary phase or residual starting materials was observed, which implies that a single amorphous structure forms in these alloys after ball milling. TEM observations were conducted in the present work for further check. In Fig.2, the selected area electron diffraction(SAED) image of $Mg_{0.9}Ti_{0.1}Ni_{0.9}Pd_{0.1}$ alloy exhibits a broad and ambiguous ring, which indicates that the long-term order structure completely disappears and the amorphous structure forms in the alloys. The other three alloys also possess the similar structures as $Mg_{0.9}Ti_{0.1}Ni_{0.9}Pd_{0.1}$ alloy by XRD and TEM analyses.

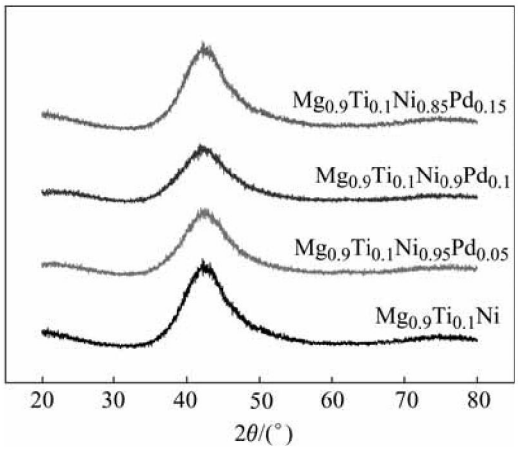

Fig.1 XRD patterns of $Mg_{0.9}Ti_{0.1}Ni_{1-x}Pd_x$ (x=0, 0.05, 0.1, 0.15) alloy powders after ball milling for 120 h

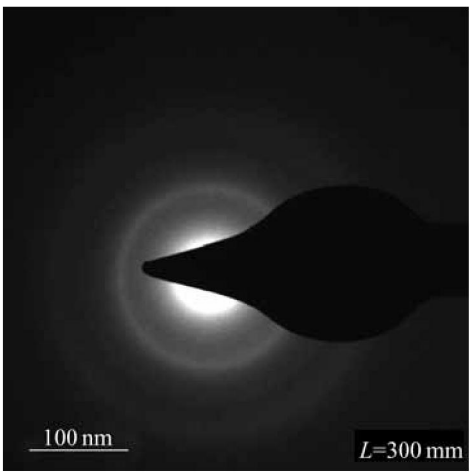

Fig.2 Selective area electron diffraction (SAED) image of $Mg_{0.9}Ti_{0.1}Ni_{0.9}Pd_{0.1}$ alloy after ball milling for 120 h

3.2 Potentiostatic discharge

For potentiostatic discharge tests the integration of $I(t)$ vs time curve represents as total charge. Thus the reacted fraction $\alpha(t)$ during the discharge can be defined as follows:

$$\alpha(t)=\frac{\int_0^t I(t)\mathrm{d}t}{\int_0^\infty I(t)\mathrm{d}t} \quad (1)$$

where $\int_0^\infty I(t)\mathrm{d}t$ is the maximum charge during the

discharge process and $\int_0^t I(t)\mathrm{d}t$ is the charge at the time of t. Fig.3 illustrates the dependence of reacted fraction $\alpha(t)$ on time for fully charged $Mg_{0.9}Ti_{0.1}Ni_{1-x}Pd_x$ (x=0, 0.05, 0.1, 0.15) electrode at various temperatures. It can be seen that the hydrogen desorption rates increase with temperature for all alloys, similar to that in gaseous hydrogen desorption of metal hydrides.

Usually, the reaction mechanism can be analyzed by fitting the obtained curves with the rate equations derived from different processes. Considering the amorphous structures of the studied alloys, several possible kinetics equations were used to fit the experimental data[16]. Table 1 summarizes the used kinetics equations and related hydrogen desorption mechanisms. In the present work, the hydrogen desorption curves of $Mg_{0.9}Ti_{0.1}Ni_{1-x}Pd_x$ (x=0, 0.05, 0.1, 0.15) electrode alloys can be fitted with good accuracy by Jander diffusion model, whose kinetics equation is

$$[1-(1-\alpha)^{1/3}]^2=kt \quad (2)$$

where α is the reacted fraction, k and t represent rate constant and time, respectively.

The relationships between $[1-(1-\alpha(t))^{1/3}]^2$ and t for $Mg_{0.9}Ti_{0.1}Ni_{1-x}Pd_x$ (x=0, 0.05, 0.1, 0.15) electrode alloys are plotted in Fig.4. The straight lines in the figure are the fitted lines of experimental data using Eqn.(2). The plots are not linear over the entire reaction range and

Table 1 Mechanisms and kinetics equations used to fit experimental data

Mechanism	Kinetics equation	r
Chemical reaction	$1-(1-\alpha)^r=kt$	1/2, 2, 3, 4, 1/4, 1/3
	$(1-\alpha)^{-2}=kt$	
	$(1-\alpha)^{-1}-1=kt$	
	$(1-\alpha)^{-1}=kt$	
	$(1-\alpha)^{-1/2}=kt$	
1-dimensional diffusion	$\alpha^2=kt$	
2-dimensional diffusion	$\alpha+(1-\alpha)\ln(1-\alpha)=kt$	
	$[1-(1-\alpha)^{1/2}]^2=kt$	
	$[1-(1-\alpha)^{1/2}]^{1/2}=kt$	
3-dimensional diffusion	$[1-(1-\alpha)^{1/3}]^2=kt$	
	$[1-(1-\alpha)^{1/3}]^{1/2}=kt$	
	$1-2\alpha/3-(1-\alpha)^{2/3}=kt$	
	$[(1+\alpha)^{1/3}-1]^2=kt$	
	$[(1-\alpha)^{(-1/3)}-1]^2=kt$	
	$(1+\alpha)^{2/3}+(1-\alpha)^{2/3}=kt$	

α denotes as reacted fraction; k and t represent rate constant and time, respectively.

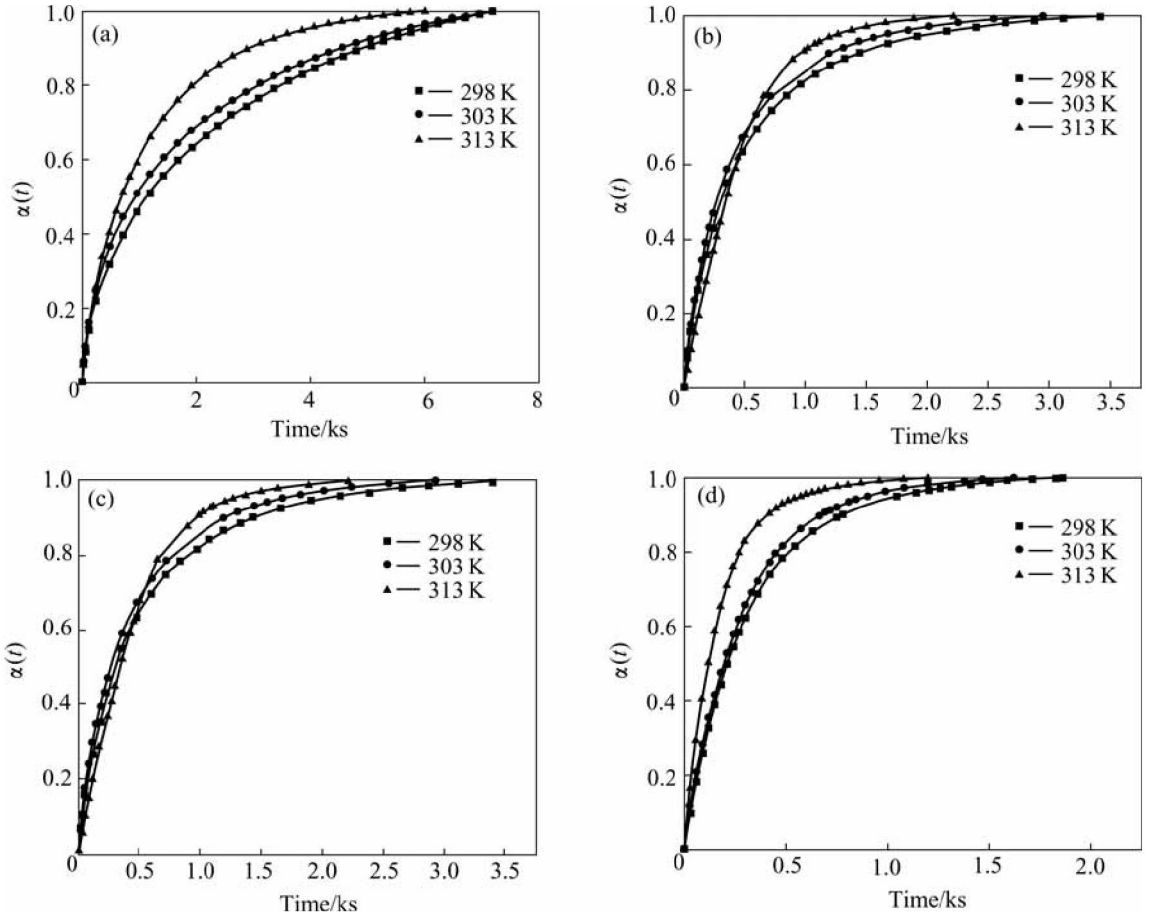

Fig.3 Dependence of reacted fraction $\alpha(t)$ on time for fully charged $Mg_{0.9}Ti_{0.1}Ni_{1-x}Pd_x$ (x=0, 0.05, 0.1, 0.15) electrode alloys at various temperatures: (a) $Mg_{0.9}Ti_{0.1}Ni$; (b) $Mg_{0.9}Ti_{0.1}Ni_{0.95}Pd_{0.05}$; (c) $Mg_{0.9}Ti_{0.1}Ni_{0.9}Pd_{0.1}$; (d) $Mg_{0.9}Ti_{0.1}Ni_{0.85}Pd_{0.15}$

a deviation from the fitted line is found at the initial stage of discharge. Such deviation is resulted from the surface charge transfer instead of 3-dimensional diffusion being the rate control step at the initial stage of discharge. However, the hydrogen diffusion almost dominates the entire discharge process for the studied alloys, which is verified with the fact that the fitted lines are close to most of the experimental data points in the figure. Similar results are obtained for the amorphous $LaNi_5$ type films[18], which is concluded that the hydrogen desorption is bulk controlled by the hydrogen diffusion in amorphous La-Ni films. The disordered structures of amorphous alloys do not possess certain channels such as grain boundaries or interfaces for rapid hydrogen diffusion[19], which results in the slow reaction kinetics and the hydrogen diffusion dominating hydrogen desorption process in this work.

The logarithmic form of Arrhenius equation is

$$\ln k=\ln k_0-(E_a/R)/T \quad (3)$$

where k is the rate constant, k_0 is the pre-exponential factor, E_a is the activation energy, R is the gas constant and T is the absolute temperature. The plots of ln$k$ vs 1 000/T for $Mg_{0.9}Ti_{0.1}Ni_{1-x}Pd_x$ (x=0, 0.05, 0.1, 0.15) electrode alloys are shown in Fig. 5. It is demonstrated that the good linear dependence exists between ln$k$ and 1 000/T. The slopes ($-E_a/R$) of the lines can be calculated and the resulted activation energies are listed in Table 2. From the table it can be seen that the activation energies of electrode alloys decrease first and then increase with the increase of Pd content.

Table 2 Relationship between activation energy of hydrogen desorption and exchange current densities of $Mg_{0.9}Ti_{0.1}Ni_{1-x}Pd_x$ (x=0, 0.05, 0.1, 0.15) electrode alloys

x	Activation energy/ (kJ·mol^{-1})	Exchange current density/ (mA·g^{-1})
0	46.2	176
0.05	34.95	303
0.1	33.40	231
0.15	24.29	185

3.3 Linear Polarization

Fig.6 indicates the linear polarization curves of $Mg_{0.9}Ti_{0.1}Ni_{1-x}Pd_x$ (x=0, 0.05, 0.1, 0.15) electrode alloys measured at 50% DOD and 303 K. It is well known that

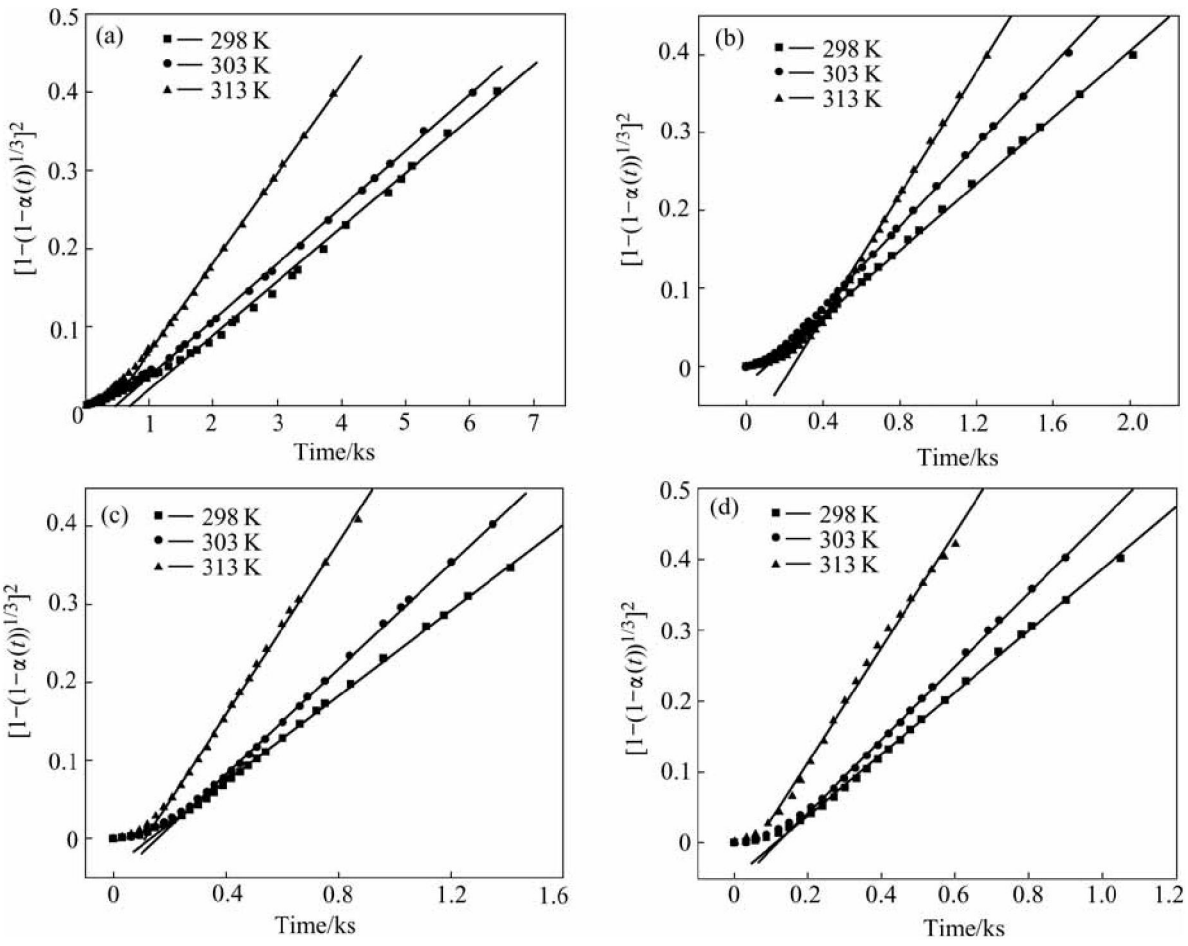

Fig.4 Relationship between $[1-(1-\alpha(t))^{1/3}]^2$ and t at various temperatures for $Mg_{0.9}Ti_{0.1}Ni_{1-x}Pd_x$ (x=0, 0.05, 0.1, 0.15) electrode alloys: (a) $Mg_{0.9}Ti_{0.1}Ni$; (b) $Mg_{0.9}Ti_{0.1}Ni_{0.95}Pd_{0.05}$; (c) $Mg_{0.9}Ti_{0.1}Ni_{0.9}Pd_{0.1}$; (d) $Mg_{0.9}Ti_{0.1}Ni_{0.85}Pd_{0.15}$

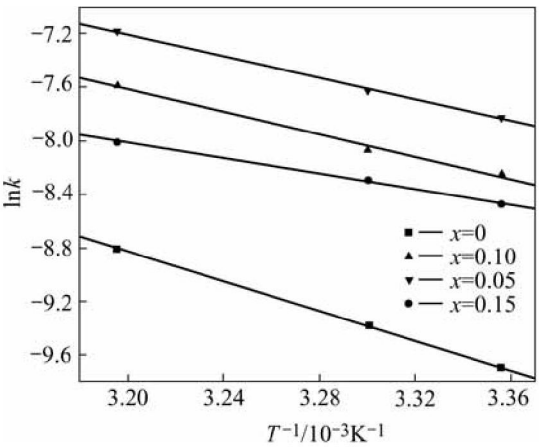

Fig.5 Plots of ln$k$ vs 1 000/T for $Mg_{0.9}Ti_{0.1}Ni_{1-x}Pd_x$ (x=0, 0.05, 0.1, 0.15) electrode alloys

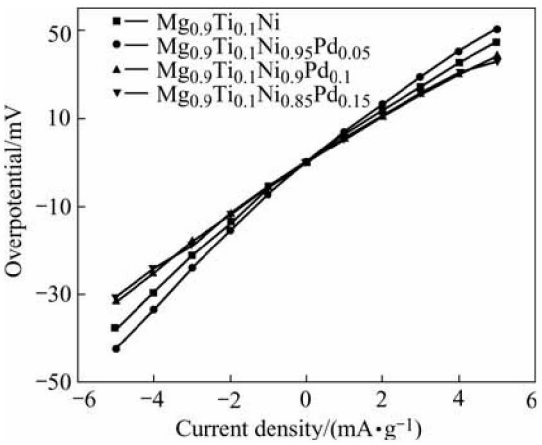

Fig.6 Linear polarization curves of $Mg_{0.9}Ti_{0.1}Ni_{1-x}Pd_x$ (x=0, 0.05, 0.1, 0.15) electrode alloys at 50% DOD and 303 K

the exchange current density I_0 can be calculated by the following equation[20]:

$$I_0=RTi/F\eta \quad (4)$$

where R, T, F, i and η stand for the gas constant, absolute temperature, Faraday constant, experimental current and overpotential, respectively. The calculated exchange current densities of the electrode alloys are also summarized in Table 2. It can be seen that the exchange currents of the electrode alloys increase first from 176 mA/g (x=0) to 303 mA/g (x=0.05) and then decrease to 185 mA/g (x=0.15) with the increase of Pd content. It is suggested that Pd plays a positive role in the hydrogen desorption of the alloys within the content range from 0 to 0.05. Excessive Pd addition results in the decline of reaction rate in this study. Previous work [21] also found that additional Pd enhanced the reaction resistance on the surface of Mg-based amorphous alloys. Therefore, the substitution of Pd for Ni caused the retardance of charge transfer on the surface of the quaternary electrode alloys in the present work. Similar phenomena were also reported by SORIAGA et al[22]. In general, the higher the exchange current is, the faster the electrochemical reaction proceeds. As we know, the larger the activation energy, the slower the reaction rate. The relationship between the activation energy and the exchange current for the electrode alloys is illustrated in Fig.7. It is demonstrated that the positive role of Pd for the hydrogen desorption is limited. When Pd content is no more than 0.05, it is helpful to accelerate the hydrogen desorption. However when its content is higher than 0.05, the desorption reaction is slowed down. On the whole, the hydrogen desorption rate is improved due to the substitution of Pd for Ni in the studied alloys.

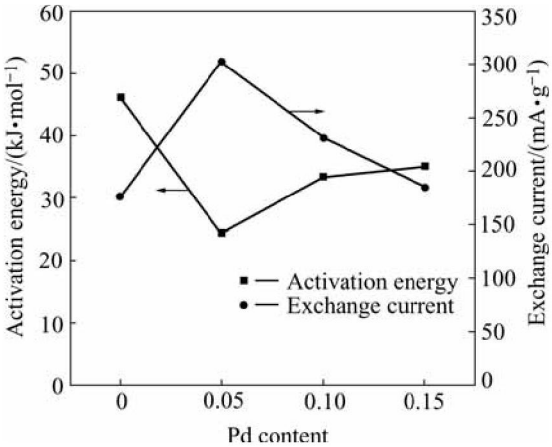

Fig.7 Relationship between activation energy of hydrogen desorption and exchange current for $Mg_{0.9}Ti_{0.1}Ni_{1-x}Pd_x$ (x=0, 0.05, 0.1, 0.15) electrode alloys

4 Conclusions

Potentiostatic discharge technique is an effective method to study the hydrogen desorption kinetics of hydrogen storage electrode alloys. The substitution of Pd for Ni of $Mg_{0.9}Ti_{0.1}Ni_{1-x}Pd_x$ (x=0, 0.05, 0.1, 0.15) electrode alloys improves the desorption kinetics to some extent. The hydrogen desorption is mainly dominated by three-dimensional hydrogen diffusion. The experimental data can be fitted well with the rate equation, $[1-(1-\alpha)^{1/3}]^2=kt$. The variation of activation energy and the exchange current with Pd content is consistent with each other. The optimum Pd content is 0.05 for the hydrogen desorption kinetics in the present study.

References

[1] LEI Yong-quan, WU Yu-ming, YANG Quan-ming, WU Jing, WANG Qi-dong. Electrochemical behaviour of some mechanically alloyed Mg-Ni-based amorphous hydrogen storage alloys [J]. Z Phys Chem Bd, 1994, 183: 379−384.

[2] ZHANG Yao, LI Shou-quan, CHEN Li-xin, LEI Yong-quan, WANG Qi-dong. Corrosion mechanism of mechanically alloyed $Mg_{50}Ni_{50}$ and $Mg_{45}Cu_5Ni_{50}$ alloys [J]. Trans Nonferrous Met Soc China, 2002, 12(2): 238−241.

[3] LIU Wei-hong, WU Hao-qing, LEI Yong-quan, WANG Qi-dong, WU Jing. Effects of substitution of other elements for nickel in mechanically alloyed $Mg_{50}Ni_{50}$ amorphous alloys used for nickel metal hydride batteries [J]. J Alloys Compd, 1997, 261(1−2): 289−294.

[4] YE H, LEI Y Q, CHEN L S, ZHANG H. Electrochemical characteristics of amorphous $Mg_{0.9}M_{0.1}Ni$ (M=Ni, Ti, Zr, Co and Si) ternary alloys prepared by mechanical alloying [J]. J Alloys Compd, 2000, 311(2): 194−199.

[5] HAN S C, LEE P S, LEE J Y, ZÜTTEL A, SCHLAPBACH L. Effects of Ti on the cycle life of amorphous MgNi-based alloy prepared by ball milling [J]. J Alloys Compd, 2000, 306(1−2): 219−226.

[6] ZHANG Yao, ZHANG Shu-kai, CHEN Li-xin, LEI Yong-quan, WANG Qi-dong. The study on the electrochemical performance of mechanically alloyed Mg-Ti-Ni-based ternary and quaternary hydrogen storage electrode alloys [J]. Int J Hydrogen Energy, 2001, 26(8): 801−806.

[7] RUGGERI S, ROUÉ L, HUOT J, SCHULZ R, AYMARD L, TARASCON J M. Properties of mechanically alloyed Mg-Ni-Ti ternary hydrogen storage alloys for Ni-MH batteries [J]. J Power Sources, 2002, 112(2): 547−556.

[8] MA T J, HATANO Y, ABE T, WATANABE K. Effects of Pd addition on electrochemical properties of MgNi [J]. J Alloys Compd, 2004, 372(1−2): 251−258.

[9] MA T J, HATANO Y, ABE T, WATANABE K. Effects of bulk modification by Pd on electrochemical properties of MgNi [J]. J Alloys Compd, 2005, 391(1−2): 313−317.

[10] TIAN Qi-feng, ZHANG Yao, CHU Hai-liang, SUN Li-xian, XU Fen, TAN Zhi-cheng, YUAN Hua-tang, ZHANG Tao. The electrochemical performances of $Mg_{0.9}Ti_{0.1}Ni_{1-x}Pd_x$ (x=0−0.15) hydrogen storage electrode alloys [J]. J Power Sources, 2006. (in press, dio: 10.1016/j.jpowsour.2006.04.061)

[11] KARTY A, GENOSSAR G J, RUDMAN P S. Hydriding and dehydriding kinetics of Mg in a Mg/Mg_2Cu eutectic alloy: Pressure sweep method [J]. J Appl Phys, 1979, 50(11): 7200−7209.

[12] HUOT J, LIANG G, BOILY S, VAN NESTE A, SCHULZ R. Structural study and hydrogen sorption kinetics of ball-milled magnesium hydride [J]. J Alloys Compd, 1999, 293−295: 495−500.

[13] LIANG G, HUOT J, BOILY S, SCHULZ R. Hydrogen desorption kinetics of a mechanically milled MgH_2+5at.%V nanocomposite [J]. J Alloys Compd, 2000, 305(1−2): 239−245.

[14] ZEPPELIN F V, REULE H, HISCHER M. Hydrogen desorption kinetics of nanostructured MgH_2 composite materials [J]. J Alloys Compd, 2002, 330−332: 723−726.

[15] BERLOUIS L E A, AGUADO R P, HALL P J, MORRIS S, CHANDRASEKARAN L, DODD S B. Dehydriding kinetics of a Mg-9.5wt%V sample studied by high pressure differential scanning calorimetry [J]. J Alloys Compd, 2003, 356−357: 584−587.

[16] LI Qian, LIN Qin, CHOU Kuo-chih, JIANG Li-jun. A study on the hydriding-dehydriding kinetics of $Mg_{1.9}Al_{0.1}Ni$ [J]. J Mater Sci, 2004, 39(1): 61−65.

[17] FENG F, HAN J W, GENG M M, NORTHWOOD D O. Hydrogen desorption kinetics of $LaNi_{4.7}Al_{0.3}$ metal hydride electrode using potentiostatic measurements [J]. Solar Energy Mater Solar Cells, 2000, 62(1−2): 51−61.

[18] CUEVAS F, HIRSCHER M. The hydrogen desorption kinetics of Pd-coated LaNi5-type films [J]. J Alloys Compd, 2000, 313: 269−275.

[19] AU M. Hydrogen storage properties of magnesium based nanostructured composite materials [J]. Materials Science and Engineering B, 2005, 117(1): 37−44.

[20] NOTTEN P H L, HOKKELING P. Double-phase hydride forming compounds—A new class of highly electrocatalytic materials [J]. J Electrochem Soc, 1991, 138(7): 1877−1885.

[21] NAKANO S, YAMAURA S, UCHINASHI S, KIMURA H, INOUE A. Effect of hydrogen absorption on the electrical resistance of melt-spun Mg-Pd and Mg-Ni-Pd amorphous alloys [J]. Mater Trans, 2004, 45(4): 1367−1370.

[22] BARSELLINI D, VISINTIN A, TRIACA W E, SORIAGA M P. Electrochemical characterization of a hydride-forming metal alloy surface-modified with palladium [J]. J Power Sources, 2003, 124(1): 309−313.

(Edited by LI Xiang-qun)